https://doi.org/10.1142/9789811280184_0017

Chapter 17

Precision SM Physics

Jan Kretzschmar*, Alexander Savin† and Mika Vesterinen‡

*University of Liverpool, U.K.
†University of Wisconsin-Madison, U.S.A.
‡University of Warwick, U.K.

1. Introduction

As the successor of the LEP e^+e^- collider at CERN, the LHC was originally conceived mainly as a discovery machine, not as much to perform *precision Standard Model measurements*. However, this notion has been challenged throughout Run 1 and Run 2, not just by the *forward precision* experiment LHCb, but also by a variety of percent- and permille-level measurements by ATLAS and CMS. Even though large data sets will be available at the end of Run 3 in 2025, the High-Luminosity phase of the LHC (HL-LHC) from 2029 is expected to bring further significant improvements to these measurements. Prospects for this program are discussed in detail in the "Yellow Report on the Physics at the HL-LHC, and Perspectives for the HE-LHC"[1] and in the more recent "Snowmass White Paper Contribution: Physics with the Phase-2 ATLAS and CMS Detectors"[2] and "Future physics potential of LHCb"[3] and we will give a synthesis of this in the following sections.

The obvious implication of the HL-LHC operation will be the larger data set available. The total integrated luminosity is expected to exceed what will be available by the end of Run 3 by a factor 10, reaching a total of 3–4 ab^{-1} for the ATLAS and CMS experiments and at least 300 fb^{-1} for LHCb. This will directly lead to improvements for measurements that are statistically limited.

A huge program of upgrades to the detectors and their data acquisition systems is required to fully exploit the increased luminosity delivered by the HL-LHC machine as is explained in this book. The high-intensity operation will come with a significant increase of the number of simultaneous pp interactions per bunch crossing (generally referred to as pile-up) up to 200. All detector systems will have to be more granular and precise, additional features such as timing measurements will be implemented, and the trigger systems need to be more capable to select the interesting collision events. Key examples of these upgrades are the inner tracking systems of ATLAS and CMS that will have higher performance and extend into the forward region $|\eta| < 4$ (as opposed to $|\eta| < 2.5$ now) and a more efficient full-software trigger for the first upgrade of LHCb. After further developments in the reconstruction algorithms, the significant increase in data volumes will also allow for a better understanding of experimental systematic uncertainties. To avoid theoretical uncertainties becoming dominant effects in measurements, the tools, calculations and supporting measurements will need continuous effort.

In the following sections we will first describe our expectations for the measurements of global SM parameters, then discuss the electroweak production of multiboson final states and precise differential cross section measurements with top quarks, jets and photons, before closing with some examples from quark flavour physics.

2. The SM parameters and global Electroweak fit

Even though the number of free parameters is often brought up as a limitation, the SM is a highly predictive theory and relations between parameters such as the masses and couplings are well known. The discovery of the Higgs boson and its precise mass measurement delivered the final input needed to overconstrain the global Electroweak fit. Exploiting the SM relations, parameters can be determined indirectly and compared to direct measurements. Any deviations observed in these comparisons will indicate the presence of new physics.

While not (yet) providing a similar diversity of EW precision observables as LEP, the masses of the W boson, m_W, and the top quark, m_t, as well as the effective mixing parameter $\sin^2\theta^{\text{lept}}_{\text{eff}}$ are those where the LHC already surpasses e^+e^- results or can be expected to do so. An update of the global fit of the EW precision observables was performed in Ref. 1 with the HEPFit package. The experimental constraints using the current and the expected

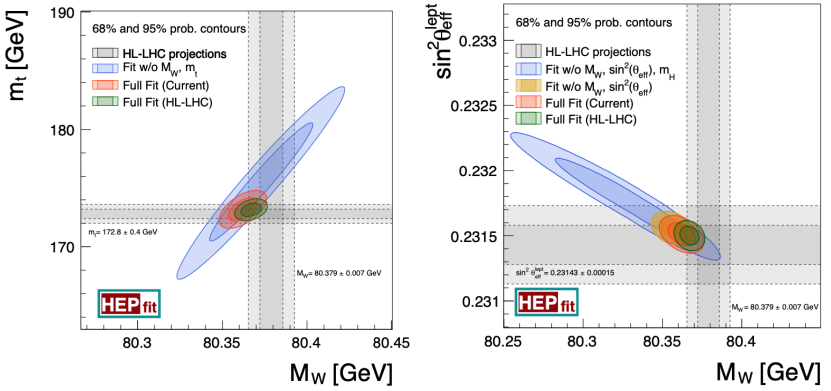

Fig. 1. Comparison of the indirect constraints on M_W and m_t with the current experimental measurements and the expected improvements at the HL-LHC (left). The same in the M_W and $\sin^2\theta_{\rm eff}^{\rm lept}$ plane (right).[1]

future HL-LHC data are shown in Fig. 1 for the relation between m_W and m_t (left) as well as m_W and $\sin^2\theta_{\rm eff}^{\rm lept}$ (right). The expected precision of the HL-LHC measurements will improve the constraints significantly and would potentially increase existing tensions between indirect and direct measurements. As also highlighted by the recent m_W measurement by CDF,[4] these measurements are able to challenge the SM and are among the main goals of the HL-LHC scientific program.

The measurement of the W-boson mass at the LHC is performed via leptonic decays to electrons or muons and the major challenge is to

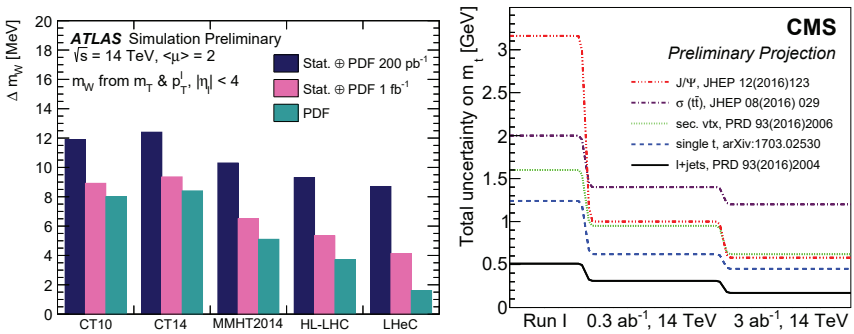

Fig. 2. Left. PDF uncertainty on the W-boson mass m_W measurement using different PDF sets.[5] Right. Total uncertainty on top quark mass (m_t) obtained with different measurement methods and their projections to the HL-LHC.[6]

overcome missing information due to the decay neutrino only visible as missing transverse momentum.[5] Previous measurements by ATLAS[7] and LHCb[8] have proved this to be possible. In fact it would appear that the requirements for this measurement — a modest sample collected at low-intensity running — are in disagreement with the HL-LHC conditions. However, the measurement can exploit the increased detector acceptance and the improved detectors. In special, low pile-up conditions with two collisions per bunch crossing on average, about 2×10^6 W boson events can be collected per week of operation. The extended detector acceptance helps to reduce the impact from parton distribution functions (PDFs) that are usually among the largest uncertainties in the measurement. The expected statistical and PDF uncertainties are summarised in Fig. 2(left) for different PDF sets. While the CT10 and CT14 PDF sets are found to give about 8 MeV uncertainty, the MMHT2014 set gives about 5 MeV. All three projected HL-LHC PDF sets with anticipated additional LHC data constraints[9] give uncertainties that are slightly lower than 4 MeV. A qualitatively different level would be reached by incorporating additional DIS data from the LHeC[10] that would halve the PDF uncertainty to about 2 MeV. Depending on the available PDF knowledge, one can expect to reach 7 MeV uncertainty or lower at the HL-LHC.

The most precise top-quark mass measurements at the LHC stem from the so-called "direct measurements" that reconstruct information from the top-quark decay products. The typical uncertainty with these methods is of the order of 500 MeV, with a recent CMS measurement reaching 380 MeV.[11] These uncertainties are dominated by the theoretical modelling and, specifically, non-perturbative QCD effects. It is thus of interest to employ a variety of alternative methods that do not rely on jet observables[6] and thus have different sensitivities to the top quark production and decay mechanisms. Instead of using the full b-jet information, one may choose final states where a b-hadron has fragmented into a J/ψ meson that decays to $\mu^+\mu^-$. The comparison of extrapolated uncertainties on the top quark mass measurements using different methods is presented in Fig. 2(right). While the "J/ψ" approach is currently significantly less precise than other methods, more data and improved systematic uncertainties are expected to bring it to the region of 500 MeV. Together with other methods this is expected to lead to a measurement of the top mass with an accuracy of a few hundred MeV at the HL-LHC.

The presence of both vector and axial-vector couplings of electroweak bosons to fermions leads to a forward-backward asymmetry A_{FB} in the

production of Drell–Yan lepton pairs that can be used to extract the effective weak mixing angle that is (at tree level) directly related to the ratio of the W and Z boson masses. First competitive measurements by ATLAS, CMS and LHCb[12–14] have been performed with Run 1 data. As this measurement is purely based on selecting a di-electron or di-muon pair, it will directly benefit from the large HL-LHC dataset, as well as the extended rapidity coverage of the central detectors.[15,16] Figure 3(left) shows an example of the A_{FB} distributions for CMS in bins of dimuon mass and rapidity for different energies and pseudorapidity acceptances. In symmetric pp collisions, A_{FB} is generated from the valence quark contributions. Extending the pseudorapidity acceptance increases the coverage for larger parton x-values in the production and reduces both the statistical and PDF uncertainties. As shown in Fig. 3(right), the PDF uncertainty restricts the precision of the measurement already for less than 100 fb^{-1}. Exploiting the PDF-dependence of the A_{FB} with dilepton rapidity and mass, one may constrain this PDF uncertainty, which hence decreases depending on the amount of data. One can expect a total uncertainty of about $12{\cdot}10^{-5}$, about a factor of two better than the current hadron collider combination. Similar conclusions have been drawn for a future measurement with LHCb.[17] Additional constraints from LHeC data have the potential to reduce this dominating PDF uncertainty by up to a factor of five.

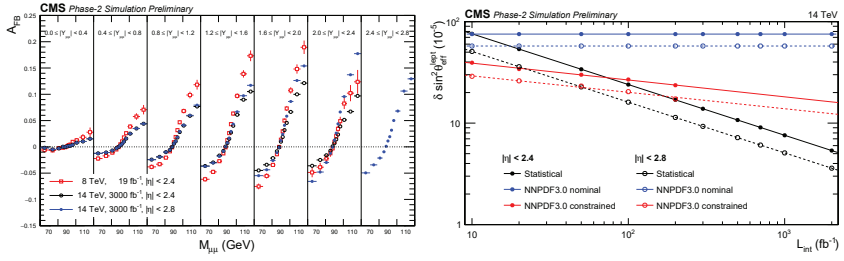

Fig. 3. Left. Forward-backward asymmetry distribution, A_{FB}, in dimuon events. Right. Projected statistical, nominal PDF and constrained PDF uncertainties for $|\eta| < 2.4$ and 2.8 acceptance selections for the muons.[15]

3. Multiboson production

The production of pairs of heavy bosons $V = W$ or Z has been an important topic of study to establish the presence of triple-gauge interactions as predicted by the SM. The frontier has now moved to the topic of purely

electroweak diboson production $VVjj$. This process class was proposed a long time ago[18,19] as being sensitive to the nature of mass generation as well as quartic-gauge interactions. It is characterised by a very low cross section and will only be conclusively investigated with data samples available at the HL-LHC. The total EW $VVjj$ production may proceed in different polarization states where each boson can be longitudinally (L) or transversely (T) polarized, leading to a total of three possibilities: LL, TL, TT. The LL component directly probes the unitarization mechanism of the vector boson scattering amplitude production through the Higgs boson.

Establishing the EW $VVjj$ production at a hadron collider over the "strong production" mechanism is already non-trivial as it requires the presence of two vector bosons in the central part of the detector and two jets separated by a large rapidity gap with reduced hadronic activity. The observation was already reported using LHC Run 2 data, starting with the golden same-charge $W^{\pm}W^{\pm}$ channel and later, also for the channels with more background, WZ and ZZ. With the increased luminosity of the HL-LHC one can expect to measure the EW $VVjj$ cross sections with a few percent uncertainty as shown in Fig. 4(left).[20] For the $W^{\pm}W^{\pm}$ channel the uncertainty at 3000 fb^{-1} is expected to reach 5%, while for WZ and ZZ 10% may be reached.

Figure 4(right) demonstrates the expected significance of the LL measurement as a function of integrated luminosity.[20] When using the WW rest frame, the sensitivity of the measurement is expected to reach $> 5\sigma$ beyond 4000 fb^{-1} such that a solid observation is expected when CMS and ATLAS will combine their results. The sensitivity of the ZZ LL

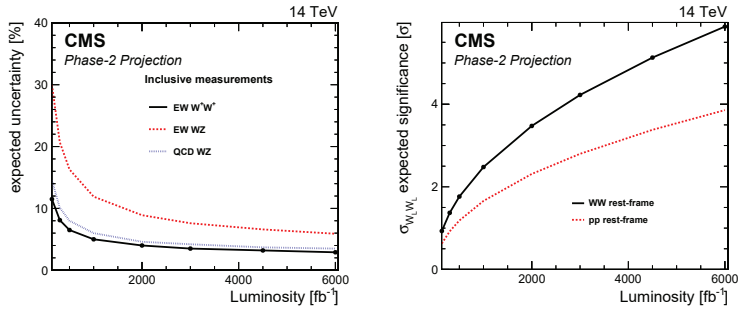

Fig. 4. Left. Projected estimated uncertainty in the EW WW, EW WZ, and QCD WZ cross section measurements as a function of the integrated luminosity. Right. Projected estimated significance for the EW W_LW_L process as a function of the integrated luminosity for the WW and parton-parton center-of-mass reference frames.[20]

measurement will be much lower. The study of triboson final states such as WWW, WWZ, WZZ has also just barely passed the observation threshold with Run 2 data and will be only fully explored at the HL-LHC.[21]

4. Differential cross sections measurements

In this section, we discuss a few examples of differential measurements that will be significantly improved in the HL-LHC phase because the data will allow an increase in precision, a reduction of the bin sizes in the *bulk phase space*, and the exploration of new phase space at higher energy or momentum.

4.1. *Measurements with top-quark pairs*

The differential $t\bar{t}$ cross-section measurements will improve at the HL-LHC because the enormous amount of data is expected to reduce dominant uncertainties related to jets. The extended η-coverage will allow fine-binned measurements at high rapidity.[22] The HL-LHC data recorded by LHCb will permit high precision measurements of asymmetries in $t\bar{t}$ production at large rapidities.

Double-differential cross-sections will be used to constrain PDF. As shown in Fig. 5(left), the uncertainties of the medium and high x gluon distribution are expected to reduce drastically when new $t\bar{t}$ data are added to the current NNPDF3.1 fit. The improvement reaches up to a factor of 10 at $x = 0.5$, the edge of the kinematic reach. Nevertheless, improving PDF uncertainties with pp data will remain difficult even at the HL-LHC. As hinted before, this can be resolved through high-luminosity ep data delivered concurrently by the LHeC as discussed in this book in Chapter 20, "Resolving the Dynamics of Partons in Protons and Nuclei".

Another example can be found by studying the kinematic properties of a top-quark pair production in association with a photon ($t\bar{t}\gamma$) that probes the electroweak $t\gamma$ coupling, provides important constrains for effective field theory and information about $t\bar{t}$ spin correlation and production charge asymmetry.[23] Deviations in the transverse momentum spectrum of the photon from the SM prediction could point to new physics through anomalous dipole moments of the top quark. Figure 5(right) illustrates how such analyses will evolve at the HL-LHC: the statistical uncertainties in all bins of the differential distribution decrease significantly and additional bins at high p_T can be added, compared to published analyses with partial Run 2

data. Also, the precise study of rare top-quark processes, such as four-top-quark production, is expected to become feasible at the HL-LHC.[24,25]

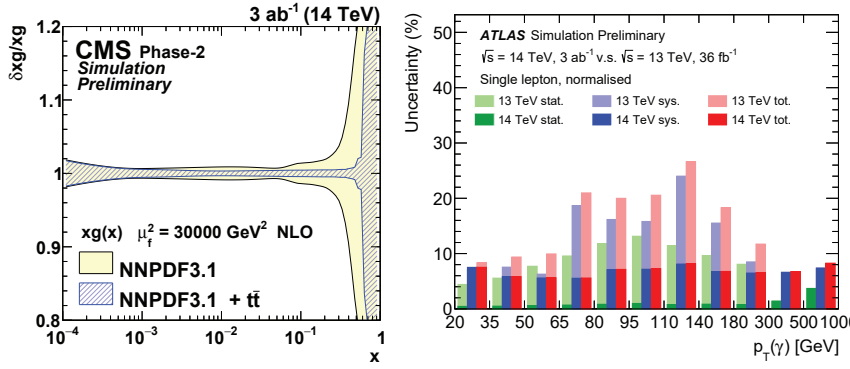

Fig. 5. Left. The relative gluon uncertainties of the original and profiled NNPDF3.1 PDF set after adding the $t\bar{t}$ information.[22] Right. Comparison of statistical/systematic/total uncertainties for the normalised differential cross-sections as a function of the photon p_T in the single-lepton channel of the $t\bar{t}\gamma$ analysis.[23]

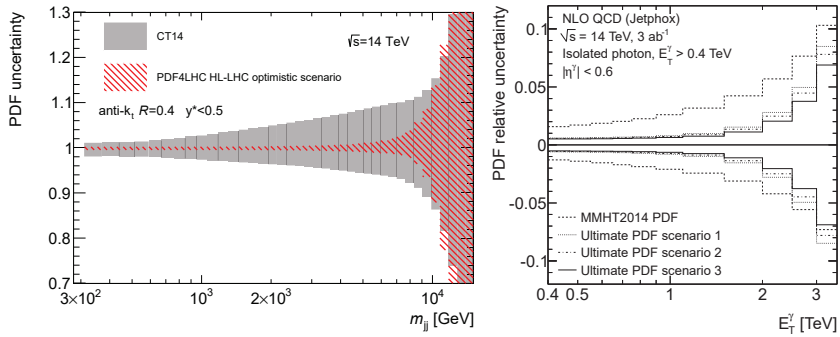

Fig. 6. Left. Comparison of the PDF uncertainty in the dijet cross sections calculated using the CT14 PDF and PDF4LHC HL-LHC sets. Right. Relative uncertainty in the predicted number of inclusive isolated photon events due to the uncertainties in the PDFs as a function of E_T^{γ}. The relative uncertainty due to the PDFs is shown for different PDF sets: the MMHT2014 PDF set (dashed lines) as well as the Ultimate PDF set in different HL-LHC scenarios.[26]

4.2. *Inclusive jet and photon measurements*

Inclusive jet production at a hadron collider is the QCD process that probes the highest accessible scales and has been used to constrain PDFs at highest x and extract the running of the strong coupling at high scales. At the HL-LHC, the accessible dijet mass range will reach up to 10 TeV, close to the kinematic limit and the highest ever reached value at colliders.[26,27] A similar case can be made for inclusive photon production where small measurement uncertainties will be reached up to many TeV. Figure 6 demonstrates how the PDF uncertainties may improve after including dijet and inclusive photon measurements into PDF fits when assuming further improvements in theory uncertainties.

5. Quark flavour physics

In the SM there are three families of fermions, distinguished by their flavour. The fermion mass hierarchy is governed by Yukawa interactions with the Higgs field. The mis-alignment between the mass and weak-interaction eigenstates of the quarks is characterised by the Cabibbo-Kobayashi-Maskawa (CKM) matrix, with its four degrees of freedom corresponding to three angles and one phase, which is the only source of CP-violation in the SM. The six quark masses and four mixing parameters are free parameters of the SM and an open question is: Whether there is a deeper explanation for the hierarchical pattern in their values. The study of quark flavour changing transitions may reveal amplitudes involving new fields with a different flavour patterns.

While previously the field of quark flavour physics was determined almost entirely by e^+e^- collision data collected at the $\Upsilon(4S)$ resonance, the first decade of the LHC has changed the landscape. The cross-section for beauty hadron production at the LHC is roughly five orders of magnitude larger at about 1 mb. Furthermore, beauty hadrons are produced inclusively, meaning all conceivable meson, baryon, or exotic bound states are available. Charmed hadrons are produced at an even higher rate. The LHCb experiment has demonstrated emphatically that high precision studies of beauty and charm hadrons is possible at the LHC with its unique instrumentation in the forward pseudorapidity range of $2 < \eta < 5$. The ATLAS and CMS experiments have contributed studies of beauty hadron decays particularly with decays into dimuon final states that are more easily triggered.

5.1. *The unitarity triangle*

The search for BSM physics in quark flavour requires the precise determination of the free CKM parameters of the SM using processes unlikely to be influenced by BSM physics, because they are dominated by tree-level amplitudes in the SM. Deviations are then searched for in processes that occur at loop-level in the SM. Six of the unitarity conditions of the CKM matrix can be represented by triangles. The triangle representing the condition $V_{ud}V_{ub}^* + V_{cd}V_{cb}^* + V_{td}V_{tb}^* = 0$ is usually referred to as *the* unitary triangle (UT). Figure 7 shows the projected constraints on the UT with data from the LHCb Upgrade II. The length of the left hand side of the triangle is determined from tree-level semileptonic decays of beauty hadrons via $b \to c$ and $b \to u$ transitions. LHCb can contribute, in particular, with decays of a wide range of beauty hadrons, having already demonstrated first observations of V_{ub} decays with B_s mesons[28] and Λ_b baryons.[29] LHCb Upgrade II will allow unprecedented precision on these rare decays and further permit studies of similar decays of B_c mesons, which are currently beyond reach.

The slope of the left hand side of the triangle corresponds to the phase $\gamma = \arg\left[\frac{V_{ud}V_{ub}^*}{V_{cd}V_{cb}^*}\right]$, which can be determined via the family of $B \to DK$ decays. These decays are mediated via tree-level $b \to u$ and $b \to c$ transitions and the interference between the corresponding amplitudes causes CP asymmetries that depend on γ. The CP asymmetries also depend on the relative magnitudes and phases of the amplitudes but these can be simultaneously determined from the data. A recent combination of measurements of CP observables in such decays from LHCb resulted in a determination of $\gamma = (63.8^{+3.5}_{-3.7})^\circ$.[30] These measurements are extremely clean since most experimental systematic uncertainties cancel very effectively. However, these decays are to fully hadronic final states, for which the trigger efficiency is a limitation of the current experiment. With the full LHCb Upgrade II dataset a determination of γ will be made possible, with a precision of around 0.3°. With the apex of the UT fixed by measurements of $|V_{ub}|/|V_{cb}|$ and γ via tree-level decays, the slope and length of the side proportional to $V_{td}V_{tb}^*$ can be determined with loop processes that are extremely sensitive to BSM physics.

5.2. *Exotic hadrons*

The first decade of the LHC has already rewritten the textbooks on bound quark states, following a proliferation of states that are indicative of $Q\bar{Q}q\bar{q}$

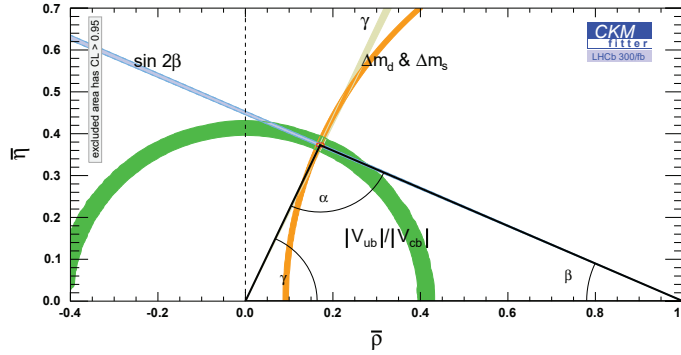

Fig. 7. A projection of the constraints on the Unitarity Triangle with 300 fb^{-1} of data from the LHCb Upgrade II.[31]

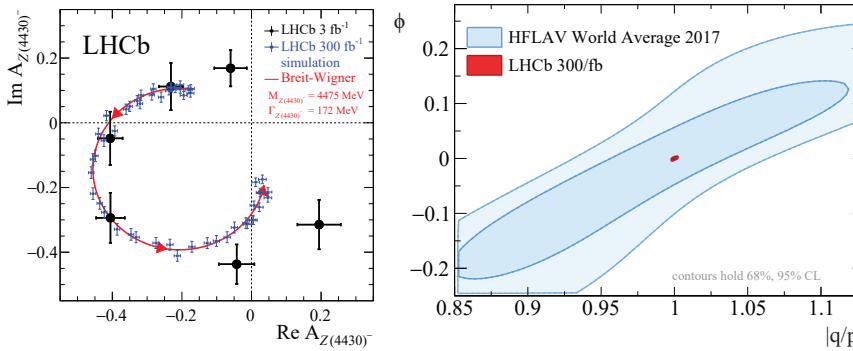

Fig. 8. Left: Argand diagram of the $Z(4430)^-$ amplitude ($A_{Z(4430)^-}$) in bins of $m^2_{\psi(2S)\pi^-}$ from a fit to the $B^0 \to \psi(2S)K^+\pi^-$ decays. The black and blue points correspond to Run I data and LHCb Upgrade II projections, respectively.[31] Right: Current and projected constraints on charm indirect CP-violation parameters are delineated by the blue and red contours, respectively.[31]

quark content; the discovery of $J/\psi p$ structures with $c\bar{c}uud$ quark content by LHCb in 2015;[32] the discovery of a doubly charmed tetraquark by LHCb in 2021.[33] The existence of such states has been anticipated since the birth of the quark model in the 1960s but a complete understanding of their dynamics requires far more experimental studies. Figure 8(left) illustrates how the characteristic resonance pattern in the Argand diagram of the $Z(4430)^-$ state could be resolved with LHCb Upgrade II dataset. A particularly interesting area that is beyond the reach of current experiments

is the search for the doubly heavy baryons Ξ_{bc} and Ω_{bc}, whose production rates are predicted to be roughly an order of magnitude lower than that of B_c mesons. The HL-LHC data offer exciting prospects for their discovery.

5.3. *Charm*

A rich set of measurements and discoveries in the charm sector has been an unexpected legacy of the first decade of the LHC. This includes LHCb's first observations of $D-\overline{D}$ oscillations in 2012[34] and CP-violation in charm decays in 2019.[35] CP-violation in charm systems is expected to be small in the SM at a rate of $\mathcal{O}(10^{-4})$ or less, but can easily be enhanced by BSM physics. The study of *indirect* CP-violation, characterised by the parameters ϕ and $|q/p|$, remains currently out of reach. However, a dramatic improvement from the HL-LHC data is expected, as shown in Fig. 8(right). This is because the measurements proceed through asymmetry observables in which uncertainties cancel to a large degree and the sensitivity is limited almost entirely by data statistics.

6. Conclusions

Without attempting to summarise all topics discussed in the preceding sections, it is clear that the scope to test the SM through precision measurements with HL-LHC data is very significant. The questions addressed are of fundamental nature, such as the structure and symmetries of the SM interactions, the mechanism for mass generation, the role of flavour, and the study of the strong interaction from lowest to highest scales.

References

1. A. Dainese et al., Report on the Physics at the HL-LHC, and Perspectives for the HE-LHC. (CERN-2019-007) (2019). URL `https://cds.cern.ch/record/2703572`.
2. ATLAS and CMS Collaborations, Snowmass White Paper Contribution: Physics with the Phase-2 ATLAS and CMS Detectors (Apr, 2022). URL `http://cds.cern.ch/record/2805993`.
3. LHCb Collaboration. Future physics potential of LHCb. Technical report, CERN, Geneva (Apr, 2022). URL `https://cds.cern.ch/record/2806113`.
4. CDF collaboration, High-precision measurement of the W boson mass with the CDF II detector, *Science.* **376** (6589), 170 (2022).
5. ATLAS Collaboration. Prospects for the measurement of the W-boson

mass at the HL- and HE-LHC. Technical Report ATL-PHYS-PUB-2018-026 (2018). URL `https://cds.cern.ch/record/2645431`.

6. CMS Collaboration, ECFA 2016: Prospects for selected standard model measurements with the CMS experiment at the High-Luminosity LHC. (CMS-PAS-FTR-16-006) (2017). URL `https://cds.cern.ch/record/2262606`.
7. ATLAS collaboration, Measurement of the W-boson mass in pp collisions at $\sqrt{s} = 7$ TeV with the ATLAS detector, *Eur. Phys. J. C.* **78** (2), 110 (2018). doi: 10.1140/epjc/s10052-017-5475-4. [Erratum: Eur. Phys. J. C 78, 898 (2018)].
8. LHCb collaboration, Measurement of the W boson mass, *JHEP.* **01**, 036 (2022). doi: 10.1007/JHEP01(2022)036.
9. R. Abdul Khalek, S. Bailey, J. Gao, L. Harland-Lang, and J. Rojo, Towards Ultimate Parton Distributions at the High-Luminosity LHC, *Eur. Phys. J. C.* **78** (11), 962 (2018). doi: 10.1140/epjc/s10052-018-6448-y.
10. P. Agostini et al., The Large Hadron-Electron Collider at the HL-LHC, *J. Phys. G.* **48** (11), 110501 (2021). doi: 10.1088/1361-6471/abf3ba.
11. CMS Collaboration, A profile likelihood approach to measure the top quark mass in the lepton+jets channel at $\sqrt{s} = 13$ TeV (2022). URL `https://cds.cern.ch/record/2806509`.
12. LHCb collaboration, Measurement of the forward-backward asymmetry in $Z/\gamma^* \to \mu^+\mu^-$ decays and determination of the effective weak mixing angle, *JHEP.* **11**, 190 (2015). doi: 10.1007/JHEP11(2015)190.
13. CMS collaboration, Measurement of the weak mixing angle using the forward-backward asymmetry of Drell-Yan events in pp collisions at 8 TeV, *Eur. Phys. J. C.* **78** (9), 701 (2018). doi: 10.1140/epjc/s10052-018-6148-7.
14. ATLAS Collaboration, Measurement of the effective leptonic weak mixing angle using electron and muon pairs from Z-boson decay in the ATLAS experiment at $\sqrt{s} = 8$ TeV (Jul, 2018). URL `https://cds.cern.ch/record/2630340`.
15. CMS Collaboration, A proposal for the measurement of the weak mixing angle at the HL-LHC. (CMS-PAS-FTR-17-001) (2017). URL `http://cds.cern.ch/record/2294888`.
16. ATLAS Collaboration, Prospect for a measurement of the Weak Mixing Angle in $pp \to Z/\gamma^* \to e^+e^-$ events with the ATLAS detector at the High Luminosity Large Hadron Collider. (ATL-PHYS-PUB-2018-037) (2018). URL `https://cds.cern.ch/record/2649330`.
17. W. J. Barter. Prospects for measurement of the weak mixing angle at LHCb. Technical report, CERN, Geneva (Nov, 2018). URL `https://cds.cern.ch/record/2647836`.
18. M. J. G. Veltman, Second Threshold in Weak Interactions, *Acta Phys. Polon. B.* **8**, 475–492 (1977).
19. B. W. Lee, C. Quigg, and H. B. Thacker, The Strength of Weak Interactions at Very High-Energies and the Higgs Boson Mass, *Phys. Rev. Lett.* **38**, 883–885 (1977). doi: 10.1103/PhysRevLett.38.883.
20. CMS Collaboration. Prospects for the measurement of vector boson scattering production in leptonic $W^\pm W^\pm$ and WZ diboson events at $\sqrt{s} =$

14 TeV at the High-Luminosity LHC. Technical Report CMS-PAS-FTR-21-001 (2021). URL https://cds.cern.ch/record/2776773.

21. ATLAS Collaboration. Prospect studies for the production of three massive vector bosons with the ATLAS detector at the High-Luminosity LHC. Technical Report ATL-PHYS-PUB-2018-030 (2018). URL https://cds.cern.ch/record/2647220.
22. CMS Collaboration. Projection of measurements of differential $t\bar{t}$ production cross sections in the e/μ+jets channels in pp collisions at the HL-LHC. Technical Report CMS-PAS-FTR-18-015 (2018). URL http://cds.cern.ch/record/2651195.
23. ATLAS Collaboration. Prospects for the measurement of $t\bar{t}\gamma$ with the upgraded ATLAS detector at the High-Luminosity LHC. Technical Report ATL-PHYS-PUB-2018-049 (2018). URL https://cds.cern.ch/record/2652168.
24. ATLAS Collaboration. HL-LHC prospects for the measurement of the Standard Model four-top-quark production cross-section. Technical Report ATL-PHYS-PUB-2018-047 (2018). URL https://cds.cern.ch/record/2651870.
25. CMS Collaboration. Expected sensitivities for $t\bar{t}t\bar{t}$ production at HL-LHC and HE-LHC. Technical Report CMS-PAS-FTR-18-031 (1900). URL http://cds.cern.ch/record/2650211.
26. ATLAS Collaboration. Prospects for jet and photon physics at the HL-LHC and HE-LHC. Technical Report ATL-PHYS-PUB-2018-051 (2018). URL https://cds.cern.ch/record/2652285.
27. CMS Collaboration. High-p_T jet measurements at the HL-LHC. CMS Physics Analysis Summary CMS-PAS-FTR-18-032 (2018). URL http://cds.cern.ch/record/2651219.
28. LHCb collaboration, First observation of the decay $B_s^0 \to K^-\mu^+\nu_\mu$ and Measurement of $|V_{ub}|/|V_{cb}|$, *Phys. Rev. Lett.* **126** (8), 081804 (2021). doi: 10.1103/PhysRevLett.126.081804.
29. LHCb collaboration, Determination of the quark coupling strength $|V_{ub}|$ using baryonic decays, *Nature Phys.* **11**, 743–747 (2015). doi: 10.1038/nphys3415.
30. Simultaneous determination of the CKM angle γ and parameters related to mixing and CP violation in the charm sector. Technical report, CERN, Geneva (2022). URL https://cds.cern.ch/record/2838029.
31. R. Aaij et al., Physics case for an LHCb Upgrade II - Opportunities in flavour physics, and beyond, in the HL-LHC era (8, 2018).
32. LHCb collaboration, Observation of $J/\psi p$ Resonances Consistent with Pentaquark States in $\Lambda_b^0 \to J/\psi K^- p$ Decays, *Phys. Rev. Lett.* **115**, 072001 (2015). doi: 10.1103/PhysRevLett.115.072001.
33. LHCb collaboration, Observation of an exotic narrow doubly charmed tetraquark (9, 2021).
34. LHCb collaboration, Observation of $D^0 - \overline{D}^0$ oscillations, *Phys. Rev. Lett.* **110** (10), 101802 (2013). doi: 10.1103/PhysRevLett.110.101802.
35. LHCb collaboration, Observation of direct CP violation in D^0 meson decays at LHCb. pp. 263–270 (2019). doi: 10.1393/ncc/i2020-20041-4.